Published in Physical Review Letters ***85****(2), 349—352 (2000).*

Measurement of Roughness of Two Interfaces of a Dielectric Film by Scattering Ellipsometry

Thomas A. Germer

Optical Technology Division, National Institute of Standards and Technology, Gaithersburg, Maryland 20899

(Received 17 March 2000)

The polarization of light scattered by oxide films thermally grown on photolithographically-generated microrough silicon surfaces was measured as functions of scattering angle. Using the predictions of first-order vector perturbation theory for scattering from interfacial roughness to interpret the results, the roughness of each interface and the correlation function between the two interfaces can be determined. The results show the spatial frequency dependence of the SiO_2/Si interface smoothening.

PACS numbers: 68.55.Jk, 42.25.Fx, 68.35.Ct, 78.66.Nk

The roughness of a buried interface is a concern to a wide variety of applications. For example, roughness of a SiO_2/Si interface at a gate oxide affects dielectric breakdown and the transport properties of carriers in the silicon [1]. Scattering from optical coatings is affected by roughness of all of the interfaces [2]. The morphology of phase separation in polymer-blend films can depend upon the topography of the underlying surface, and can manifest itself in additional topography of the top interface [3]. Despite the importance of roughness in the performance of dielectric films and coatings, *in situ* measurement of the morphology of each of the two interfaces of a film has been difficult. X-ray and neutron scattering measurements can be used to determined roughness parameters, but the analyses require extensive modeling, with the results being model dependent [4]. Spectroscopic ellipsometry in the specular direction can be used to determine interfacial widths, but lacks the ability to determine the spatial-frequency spectrum of that roughness [5].

In this Letter, measurements of the intensity and polarization of light elastically scattered from rough dielectric layers are reported. These measurements demonstrate that ellipsometry, a commonly used technique for measuring film thickness and interfacial width, can be extended to the scattering regime, yielding film roughness and cross-correlation statistics. The only parameters required for the analysis are the optical constants of the substrate and film, and the thickness of the film, which can be extracted from data obtained in the specular condition. Therefore, light scattering ellipsometry enables a complete non-contact, non-destructive characterization of the roughnesses of both interfaces.

It is widely known that the intensity of light elastically scattered by a bare surface in the smooth surface limit is proportional to the power spectral density (PSD) function, $|Z(\mathbf{q})|^2$, of the surface height $z(x,y)$ [6]. When the only source of scattering is variation of the height of the surface, when those surface height variations are small compared to the wavelength of the light, and when the surface slopes are much less than unity, first-order

vector perturbation theory predicts that the differential Stokes-vector power scattered into a specific direction, defined by polar angle θ_r and azimuthal (out-of-plane) angle ϕ_r, is given by [7]

$$d\mathbf{P}_s = (16\pi^2/\lambda^4)\cos\theta_i \cos^2\theta_r \left|Z(\mathbf{q})\right|^2 \mathbf{Q}\,\mathbf{P}_i\, d\Omega, \qquad (1)$$

where θ_i is the incident polar angle, $Z(\mathbf{q})$ is the two-dimensional Fourier transform of $z(x,y)$, $\mathbf{P}_i$ is the incident Stokes-vector power, $d\Omega$ is the differential solid angle of collection, and $\mathbf{Q} = \mathbf{Q}(\theta_i, \theta_r, \phi_r)$ is a Mueller matrix, which depends upon the optical constants of the surrounding media and converges to the sample reflectance matrix when $\theta_i = \theta_r$ and $\phi_r = 0$ (the specular condition). The Fourier transform is evaluated at a surface wavevector $\mathbf{q}$, whose components are determined by the Bragg condition:

$$\begin{aligned} q_x &= k(\sin\theta_r \cos\phi_r - \sin\theta_i) \\ q_y &= k \sin\theta_r \sin\phi_r \end{aligned} \qquad (2)$$

where $k = 2\pi/\lambda$. Eqs. (1) and (2) are used to extract surface roughness from angle-resolved scattering data over the entire electromagnetic spectrum.

The first-order vector perturbation theory has been extended to allow for multiple interfaces [8,9]. The extended theory predicts a dependence of the scattering on the PSDs of each interface and the degree of phase correlation between the interfaces. Measurements have been performed on optical multilayers demonstrating application of the theory in the limits of high or low correlation [2]. These studies have primarily relied on the presence or absence of interference features in the angular distribution of intensity that exist due to the interference of the fields scattered from each interface and only exist for optically thick films or multilayers. Angle-resolved light scattering at three different wavelengths has been employed to characterize a single dielectric layer, but it was found that not enough information is available to extract the roughness of each interface and the cross-correlation statistics [10].

Recent work has demonstrated that the polarization of scattered light contains information that allows the source of scattering, be it surface roughness, subsurface defects, or particulate contamination, to be identified [11,12]. For example, measurements testing the consistency of the polarization with the matrix $\mathbf{Q}$ can be used to validate the use of Eqs. (1) and (2) [11]. The vector perturbation theory for light scattering from a rough dielectric film predicts a polarization dependence to the light scattering, which, like the amplitude, depends upon the roughness of each interface and the correlation between the interfaces. Calculations for the polarization of light scattered by the interfaces of a dielectric film have been performed for optical multilayers, and these results have been compared to experimental data in specific limits [13]. The author, however, knows of no case where the roughness parameters have been extracted from experimental data.

The samples used to demonstrate the application of light scattering ellipsometry consisted of two microfabricated silicon wafers, each having a pseudorandom distribution of two diameters of circular shallow pits (nominal diameters of 1.31 μm and 1.76 μm, depths of 8 nm, and density of 8×10^4 mm^{-2}). Oxide layers were thermally grown on each of these wafers with thicknesses of 10.3 nm and 52 nm, respectively, as determined by specular ellipsometry. The roughnesses of the two interfaces on each sample are expected to be coherent and identical, at least for small $\mathbf{q}$. A previous study showed that the polarization of light scattered by similar samples before growth of the oxide layers was consistent with scattering from microroughness [11]. A large amount of data

characterizing interfacial roughness in the air/SiO_2/Si system exists in the literature [5,14,15,16].

Light of wavelength λ (633 nm, 532 nm, 442 nm, or 325 nm) was incident onto each sample at an angle of θ_i (45°, 60°, or 68°). Light scattered into a solid angle dΩ (1.39×10^{-4} sr or 2.87×10^{-6} sr) defined by a polar angle of θ_r (= θ_i) and azimuthal angle ϕ_r is analyzed as a function of ϕ_r. The incident light is linearly-polarized at an angle given by $\eta_i = \pi/4 + \phi_r/2$, with respect to *s*-polarization. The out-of-plane geometry with $\eta_i = \pi/2$ (*p*-polarized) has been shown to maximize the differentiation between different scattering mechanisms at $\phi_r = \pi/2$ [11]. By employing $\eta_i = \pi/4$ for $\phi_r = 0$, $\eta_i = 3\pi/4$ for $\phi_r = \pi$, and continuously varying between these limits, we improve the differentiation for a wider range of ϕ_r. The polarization of the scattered light is measured by rotating a quarter-wave retarder, followed by a linear polarizer, in front of the detector. A detailed description of the instrument can be found elsewhere [17].

Figure 1 shows a representative measurement of polarization as a function of ϕ_r. The polarizations are represented by the principal angle that the polarization ellipse makes with respect to *s*-polarization, η, the degree of circular polarization, P_C, and the degree of polarization, P. It is straightforward to show that these parameters fully describe the polarization and map onto the usual Stokes parameters. The uncertainties in the data are dominated by statistical sources and are thus similar to the point-to-point variations observable in the data.

The scattering from the *i*-th interface can be calculated using first-order vector perturbation theory [8], yielding a scattered electric field $\mathbf{A}_i Z_i$, where $\mathbf{A}_i$ is a complex (Jones) vector, and Z_i is the Fourier transform of the surface height function, evaluated at the surface vector $\mathbf{q}$ given by Eq. (2). The vector $\mathbf{A}_i$ depends upon the film thickness, the optical constants of the film and substrate, the wavelength, the incident polarization, and the scattering geometry. The Stokes vector power $\mathbf{P}_s$ describing the net scattering from both interfaces is then given by

$$\mathbf{P}_s = \mathbf{S}(\mathbf{A}_1 Z_1 + \mathbf{A}_2 Z_2), \tag{3}$$

where $\mathbf{S}(\mathbf{X})$ is the Stokes vector representation [18] of the Jones vector $\mathbf{X}$, and subscripts 1 and 2 denote the SiO_2/Si and the air/SiO_2 interfaces, respectively. If we let $Z_2 = \chi Z_1$, and assume $C \equiv \langle \chi/|\chi| \rangle$ is real, then Eq. (3) can be written as

$$\mathbf{P}_s = \{(1-C)[\mathbf{S}(\mathbf{A}_1) + \mathbf{S}(|\chi|\mathbf{A}_2)] + C\mathbf{S}(\mathbf{A}_1 + |\chi|\mathbf{A}_2)\}|Z_1|^2. \tag{4}$$

Eq. (4) indicates that the ratio of the magnitudes of the interfacial roughness, $|\chi|$, and the degree of phase correlation between the interfaces, C, determine the polarization state of the scattered light. As long as no degeneracies exist, the measurable polarization can be inverted to yield these parameters.

Curves (a)—(d) shown in Fig. 1 show the predicted behavior for the four limiting cases of correlated and equal roughness ($|\chi| = 1$, $C = 1$), uncorrelated but equal roughness ($|\chi| = 1$, $C = 0$), top interface roughness ($\lim |\chi| \to \infty$), and bottom interface roughness ($|\chi| = 0$). Only for the case of uncorrelated roughness is any depolarization predicted. While the data follow the correlated and equal roughness model for small angles ($\phi_r < 10°$), they deviate significantly for higher angles.

The parameters η, P_C, and P are fit to Eq. (4), letting $|\chi|$ and C be adjustable parameters, constrained to be in the ranges (0, ∞) and (–1, 1), respectively. The resulting fits follow very close to the data shown in Fig. 1. Figure 2 shows $|\chi|$ and C extracted from the fits for both samples using measurements taken with λ = 532 nm and $\theta_i = \theta_r$ =

45°, 60°, and 68°. The 90 % confidence limit uncertainties in both extracted parameters are approximately 0.04, or the point-to-point fluctuations in the data, whichever is larger. Fits obtained with measurements at 325 nm, 442 nm, and 633 nm are consistent with those shown in Fig. 2. The agreement between the different wavelengths and incident angles suggests that the analysis is valid.

For both the 10.3 nm and the 52 nm oxide samples, the two interfaces appear to be highly correlated ($C \sim 1$) and, for small periodicities ($|\mathbf{q}|/2\pi < 0.5\ \mu m^{-1}$), the two surfaces have equal amplitudes ($|\chi| \sim 1$). This result comes as no surprise, since the oxidation process should be uniform on long length scales. The 10.3 nm oxide sample shows this high degree of conformity for all the periodicities probed. On the other hand, the 52 nm oxide shows a noticeable deviation of $|\chi| > 1$, indicating either roughening of the top interface or smoothening of the buried interface. This mismatched amplitude does not follow any features in the degree of correlation between the two surfaces.

Once the parameters $|\chi|$ and C are extracted from the polarization data, Eq. (4) allows the intensity of the scattered light to be immediately converted to the PSD ($|Z_i|^2$) of each interface. Figure 3 shows the resulting PSDs for the 52 nm film measured with $\lambda = 532$ nm. The results for the 10.3 nm film are similar on the scale shown, except that both interfaces are nearly identical. The curve shown in Fig. 3 shows the results of a calculation of the scattering from a random distribution of the two circular pits having their nominal diameters and densities, and shows structure resulting from two Airy diffraction patterns. The imperfect match between the experimentally measured PSDs and the nominal curve may be combined results from the lithography process that produced the structure, their pseudorandom distribution on the surface (one of each diameter, nonoverlapping, per 5 μm × 5 μm square on the surface), and the film growth process. Aside from the smoothly varying differences between the two interfaces, the data in Fig. 3 also show a shift in a local minimum near 2.7 μm^{-1}, which is near the fourth zero of the diffraction from the 1.76 μm pits and the third zero from the 1.31 μm pits. This shift is a result of the pits in the buried interface having a larger diameter than those of the exposed interface. If the interfaces are correlated to one another, and if a linear response theory were to apply [19], the transfer function $\chi(\mathbf{q})$ should be independent of either of the $Z_i(\mathbf{q})$. The presence of this shift suggests that the transfer function depends upon $Z_i(\mathbf{q})$, so that a linear response theory would not completely describe the smoothening process.

Interfacial smoothening associated with the growth of SiO_2 has been measured in the past, using atomic force microscopy (AFM) with destructive removal of the oxide [14,16], spectroscopic ellipsometry [5,16], and x-ray scattering [15]. While AFM probes length scales much shorter than those presented in this work, it cannot measure the degree of correlation between the interfaces and cannot discern the level of relative roughness variation obtainable by the light scattering ellipsometry method. Spectroscopic ellipsometry can be used to determine interfacial widths, but not the **q**-dependence of the roughness function. The x-ray studies[15] were carried out in a manner which is sensitive to interfacial width and did not yield **q**-dependent information. The results of the AFM, spectroscopic ellipsometry, and x-ray scattering studies, however, qualitatively agree with those presented here: the buried interface is smoother than the top interface, and the relative smoothness increases with thicker layers.

In this Letter, we have presented an ellipsometric scattering measurement for a dielectric film. The results demonstrate that these measurements permit a simultaneous

measurement of the roughness of two interfaces and the correlation between the two interfaces as functions of spatial frequency, without requiring contact with the sample. This technique should prove valuable for studying the growth or deposition morphology for a wide variety of transparent films on surfaces.

The author would like to thank Bradley Scheer of VLSI Standards, Inc. [20] for providing the samples.

REFERENCES

[1] T. Ohmi, et al., IEEE Trans. Electron Device **39**, 537 (1992).

[2] C. Amra, C. Grèzes-Besset, and L. Bruel, Appl. Opt. **32**, 5492 (1993); C. Amra, J. H. Apfel, and E. Pelletier, Appl. Opt. **31**, 3134 (1992); C. Amra, Appl. Opt. **32**, 5481 (1993).

[3] A. Karim, et al., Phys. Rev. E **57**, R6273 (1998).

[4] V. Holý, and T. Baumbach, Phys. Rev. B **49**, 10668 (1994).

[5] V. A. Yakovlev and E. A. Irene, J. Electrochem. Soc. **139**, 1450 (1992); V. A. Yakovlev, Q. Liu, and E. A. Irene, J. Vac. Sci. Technol. A **10**, 427 (1992); C. Zhao, P. R. Lefebvre, and E. A. Irene, Thin Solid Films **313-314**, 286 (1998).

[6] See, for example, P. Beckmann and A. Spizzichino, *The Scattering of Electromagnetic Waves from Rough Surfaces*, (Pergamon, Oxford, 1963).

[7] S. O. Rice, Comm. Pure and Appl. Math. **4**, 351 (1951); D. E. Barrick, *Radar Cross Section Handbook* (Plenum, New York, 1970).

[8] J. M. Elson, J. Opt. Soc. Am. **66**, 682 (1976); J. M. Elson, J. Opt. Soc. Am. A **12**, 729 (1995); J. M. Elson, Appl. Opt. **16**, 2873 (1977).

[9] E. Kröger and E. Kretschmann, Z. Physik **237**, 1 (1970).

[10] D. Rönnow, Opt. Eng. **37**, 696 (1998).

[11] T. A. Germer, C. C. Asmail, and B. W. Scheer, Opt. Lett. **22**, 1284 (1997); T. A. Germer, Appl. Opt. **36**, 8798 (1997); T. A. Germer and C. C. Asmail, J. Opt. Soc. Am. A **16**, 1326 (1999).

[12] L. Sung, G. W. Mulholland, and T. A. Germer, Opt. Lett. **24**, 866 (1999).

[13] C. Deumié, H. Giovannini, and C. Amra, Appl. Opt. **35**, 5600 (1996).

[14] S. J. Fang, W. Chen, T. Yamanaka, and C. R. Helms, J. Electrochem. Soc. **144**, 2886 (1997), and references therein.

[15] M.-T. Tang, *et al*., Appl. Phys. Lett. **62**, 3144 (1993); M.-T. Tang, *et al*., Appl. Phys. Lett. **64**, 748 (1994); J. L. Dawson, *et al*., J. Appl. Phys. **77**, 4746 (1995);

[16] Q. Liu, *et al.*, J. Vac. Sci. Technol. **13**, 1977 (1995); L. Lai and E. A. Irene, J. Appl. Phys. **86**, 1729 (1999).

[17] T. A. Germer, and C. C. Asmail, Rev. Sci. Instrum. **70**, 3688 (1999).

[18] R. M. A. Azzam and N. M. Bashara, *Ellipsometry and Polarized Light* (Elsevier, Amsterdam, 1987).

[19] M. O. Robbins, D. Andelman, and J.-F. Joanny, Phys. Rev. A **43**, 4344 (1991).

[20] Certain commercial equipment, instruments, or materials are identified in this paper in order to specify the experimental procedure adequately. Such identification is not intended to imply recommendation or endorsement by the National Institute of Standards and Technology, nor is it intended to imply that the materials or equipment identified are necessarily the best available for the purpose.

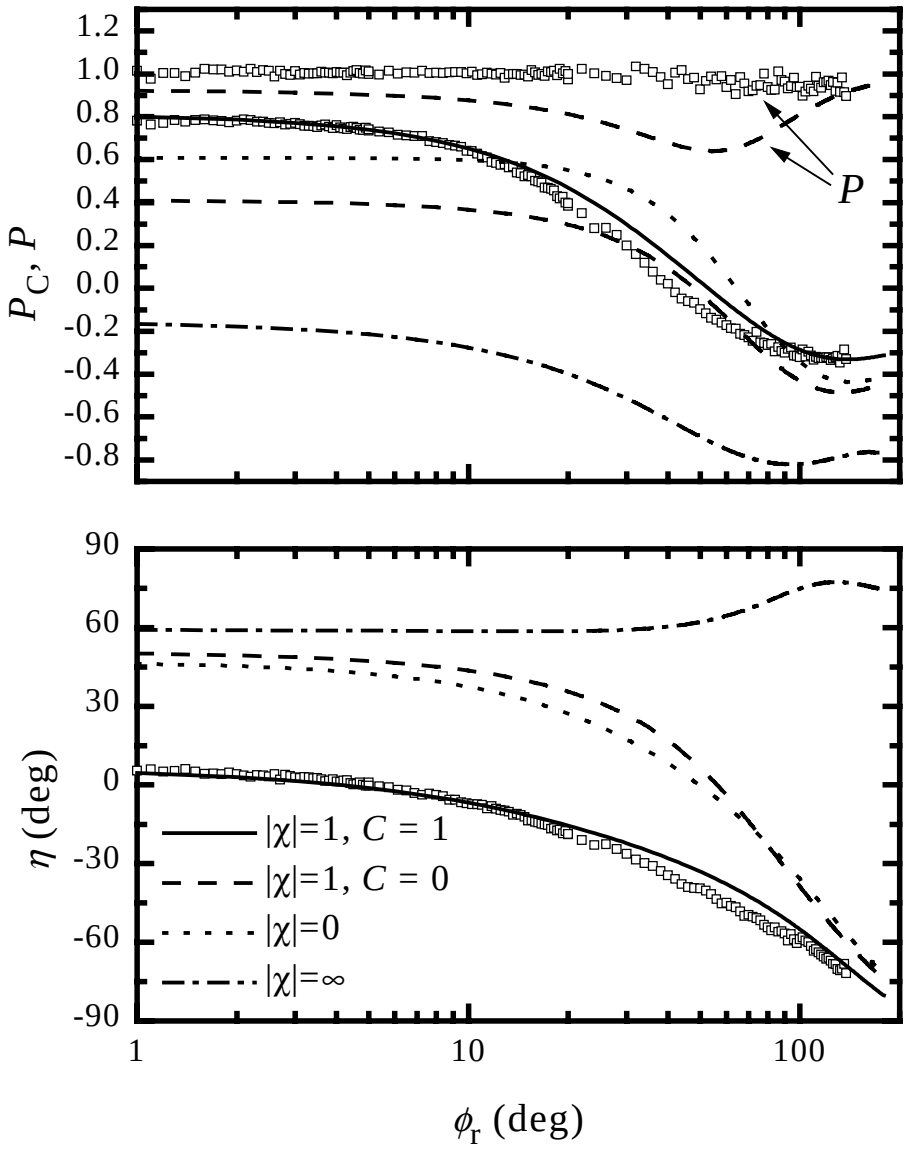

FIG. 1 Polarization of scattered light [(top) P_C and P, and (bottom) η] measured for the 52 nm SiO_2 film on Si, using λ = 532 nm, and $\theta_i = \theta_r$ = 68°. The curves represent the theory in four different limits. The theory for C = 1 predicts P = 1.

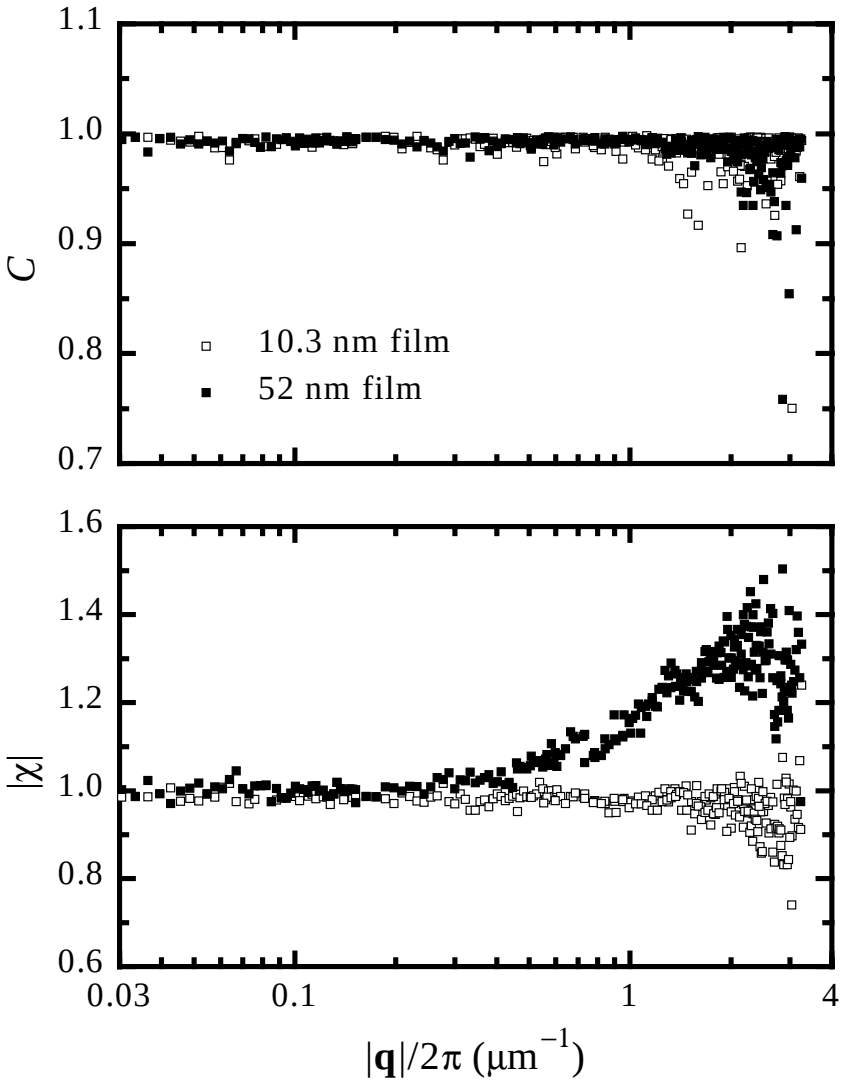

FIG. 2 Cross-interface roughness parameters, $|\chi|$ and C, extracted from the measurements using $\lambda = 532$ nm and $\theta_i = \theta_r = 45°$, 60°, and 68°. Symbols represent results for the (open) 10.3 nm film and (closed) 52 nm film.

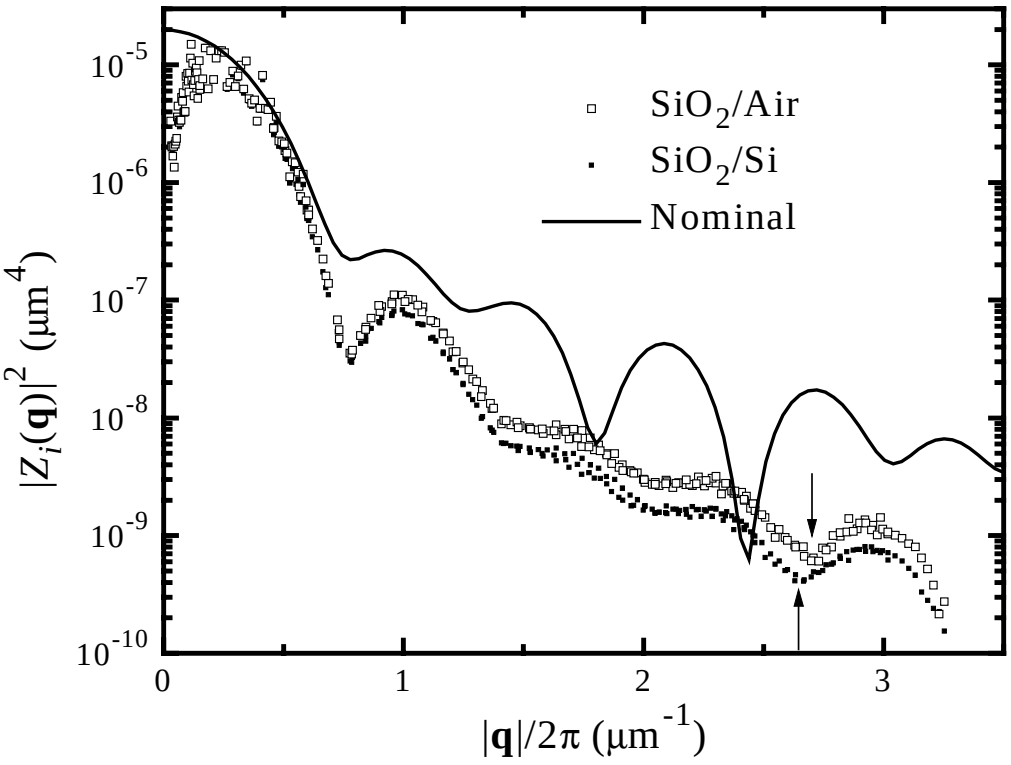

FIG. 3 The power spectral density function of each interface of the 52 nm film extracted from the amplitude of scattering. The curve represents the ideal case of two incoherent circular pits with their nominal diameters. The arrows point to a local minimum whose location is different for the two interfaces.